Supplementary Information: Phase transitions of fluorotelomer alcohols at the water|alkane interface studied via molecular dynamics simulation

Stephen A. Burrows, Jang Won Shon, Boyan Peychev,
Radomir I. Slavchov*, Stoyan K. Smoukov*

January 31, 2024

1 Computation of dihedral angle

$\mathbf{r}_1$, $\mathbf{r}_2$, $\mathbf{r}_3$ and $\mathbf{r}_4$ are the position vectors of the four atoms in the chain comprising the dihedral. Firstly the atomic positions are converted to bond vectors, such that $\mathbf{b}_1 = \mathbf{r}_2 - \mathbf{r}_1$, $\mathbf{b}_2 = \mathbf{r}_3 - \mathbf{r}_2$ and $\mathbf{b}_3 = \mathbf{r}_4 - \mathbf{r}_3$. Then, the following unit vectors are calculated, which are normal to the blue and red planes in Figure S1, respectively.

$$\mathbf{c}_1 = \frac{\mathbf{b}_1 \times \mathbf{b}_2}{|\mathbf{b}_1 \times \mathbf{b}_2|} \ , \tag{S1}$$

$$\mathbf{c}_2 = \frac{\mathbf{b}_2 \times \mathbf{b}_3}{|\mathbf{b}_2 \times \mathbf{b}_3|} \ . \tag{S2}$$

A third vector, $\mathbf{d}$ is also computed which is orthogonal to $\mathbf{c}_2$ and $\mathbf{b}_2$,

$$\mathbf{d} = \frac{\mathbf{c}_2 \times \mathbf{b}_2}{|\mathbf{b}_2 \times \mathbf{c}_1|} \ . \tag{S3}$$

$\mathbf{c}_2$ and $\mathbf{d}$ form an orthogonal basis in which $\mathbf{c}_1$ has components x and y,

$$x = \mathbf{c}_1 \cdot \mathbf{c}_2 \ , \tag{S4}$$

$$y = \mathbf{c}_1 \cdot \mathbf{d} \ .$$

Finally, the dihedral angle ϕ is computed using the two-argument atan2 function

$$\phi = \mathrm{atan2}(y, x) \ . \tag{S5}$$

The atan2 function returns an angle in the range $[-\pi, \ \pi]$ and is needed to differentiate between positive and negative angles and therefore gauche+ and gauche- dihedrals. If the angle between

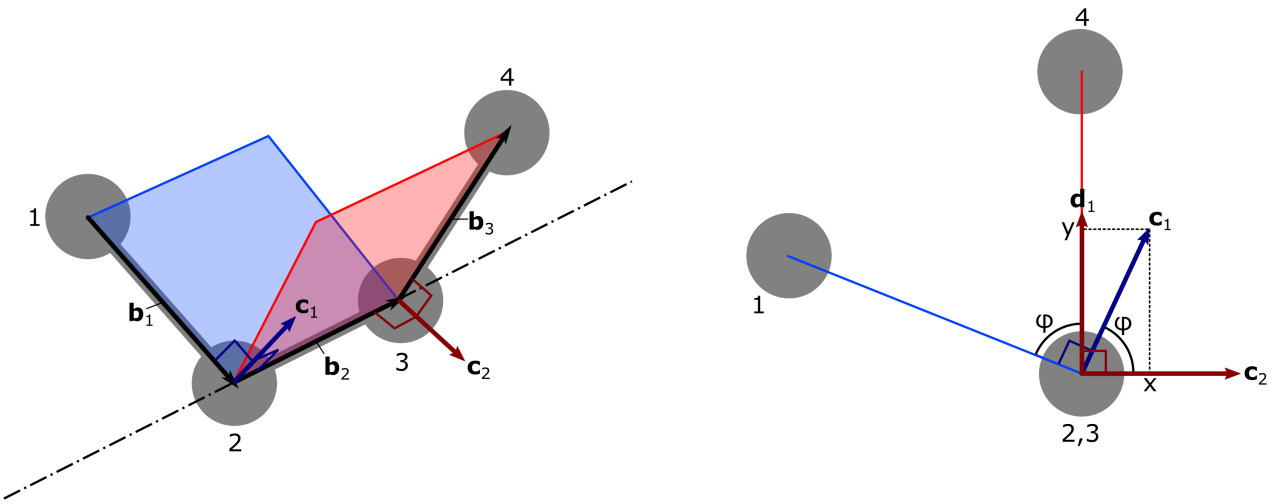

Figure S1: Vectors used in computation of the dihedral angle ϕ for a chain of four atoms.

$\mathbf{c}_1$ and $\mathbf{c}_2$ is computed simply using the dot product and inverse cosine, the result will always be positive and in the range $[0,\ \pi]$.

2 Heterogeneous monolayers

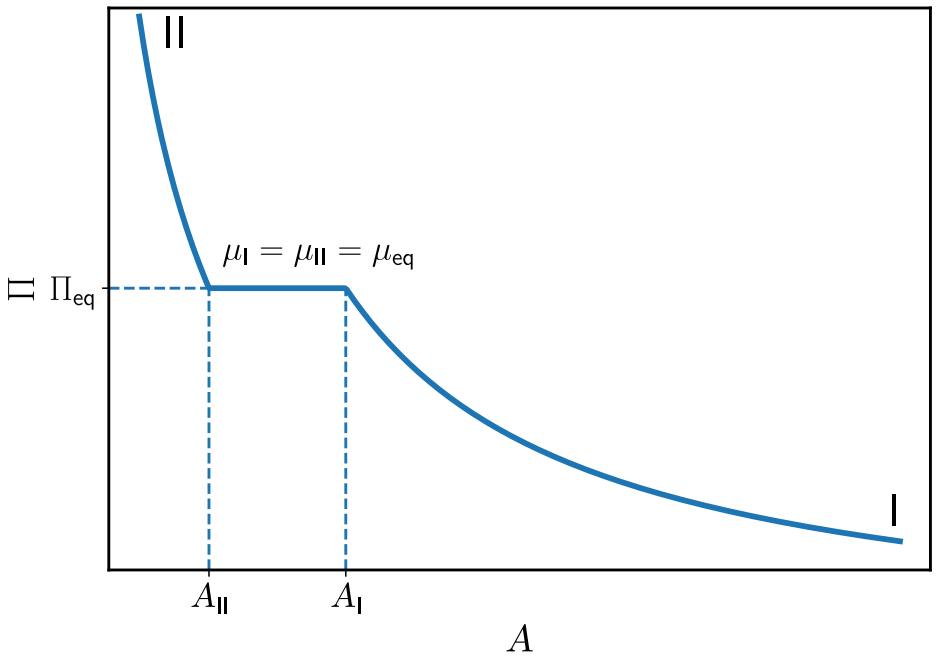

Figure S2: A textbook compression isotherm with a first order phase transition between I and II and $\tau = 0$.

Figure S2-left shows the classical textbook picture of a monolayer going through a phase transition from phase I to phase II upon contraction. At a critical area per molecule A_{I} the chemical potential of the two phases intersects and the phase transition begins. The process continues until the whole monolayer is in phase II, i.e. A_{II}. In the meantime the interfacial

pressure and the chemical potential are constant; Π_{eq} and μ_{eq}. In the region between A_{I} and A_{II} the monolayer is intrinsically heterogeneous. The constant interfacial pressure is contingent on the negligible phase line tension τ between the two phases. The line tension τ is the energy required to create a unit of phase line. The simplest type of heterogeneous monolayer is a single circular domain floating inside the continuous phase (see Figure S3). The condition of mechanical equilibrium requires that

$$\sigma_{\mathrm{c}} = \sigma_{\mathrm{d}} + \frac{\tau}{R}, \tag{S6}$$

where R is the radius of the circular domain. The indices d and c designate between the dispersed (the circular domain) and continuous phase. The condition of chemical equilibrium requires that $\mu_{\mathrm{c}} = \mu_{\mathrm{d}}$. However, unlike the simplified classical picture, the non-constant interfacial tension would generally lead to non-constant chemical potential. We can assume that the area per molecule in the two phases is constant irrespective of the ratio between the two, i.e. $A_{\mathrm{c}} = \text{const.}$ and $A_{\mathrm{d}} = \text{const.}$. Then the chemical potential of each phase can be found from the Gibbs' isotherm $\mathrm{d}\sigma = -1/A\ \mathrm{d}\mu$:

$$\mu_i = \mu_{\mathrm{eq}} - A_i(\sigma_i - \sigma_{\mathrm{eq}}), \tag{S7}$$

where i is either d or c. The subscript eq designates the values of the parameters at zero curvature, i.e. negligible contribution of the phase line. Combining the condition of chemical equilibrium, equation S6, and equation S7, we can find the surface tension of each phase as a function of the radius of the domain

$$\sigma_{\mathrm{c}} = \sigma_{\mathrm{eq}} - \frac{A_{\mathrm{d}}}{A_{\mathrm{c}} - A_{\mathrm{d}}}\frac{\tau}{R}, \tag{S8}$$

$$\sigma_{\mathrm{d}} = \sigma_{\mathrm{eq}} - \frac{A_{\mathrm{c}}}{A_{\mathrm{c}} - A_{\mathrm{d}}}\frac{\tau}{R}. \tag{S9}$$

Unfortunately, it is not immediately obvious how equations S8 and S9 relate to the interfacial tension/pressure that is experimentally measured or simulated for that matter. The interfacial tension that GROMACS calculates is an average over the whole interface. Therefore, we can write

$$\sigma = \frac{a_{\mathrm{c}}}{a}\sigma_{\mathrm{c}} + \frac{a_{\mathrm{d}}}{a}\sigma_{\mathrm{d}} + \frac{L}{a}\tau, \tag{S10}$$

a is the area of the monolayer, a_i is the area occupied by the respective phase and L is the length of the phase line. Such a relationship could also be valid for the experimentally measured surface tension, depending on the method used. From equation S6 and the last two results, we can get

$$\sigma = \sigma_{\mathrm{eq}} - \frac{A_{\mathrm{d}}}{A_{\mathrm{c}} - A_{\mathrm{d}}}\frac{\tau}{R} + \frac{\pi R}{a}\tau. \tag{S11}$$

Note that, at a constant ratio d to c, the second and third terms both scale inversely proportional to the linear size of the system. For a big enough system the terms proportional to the line

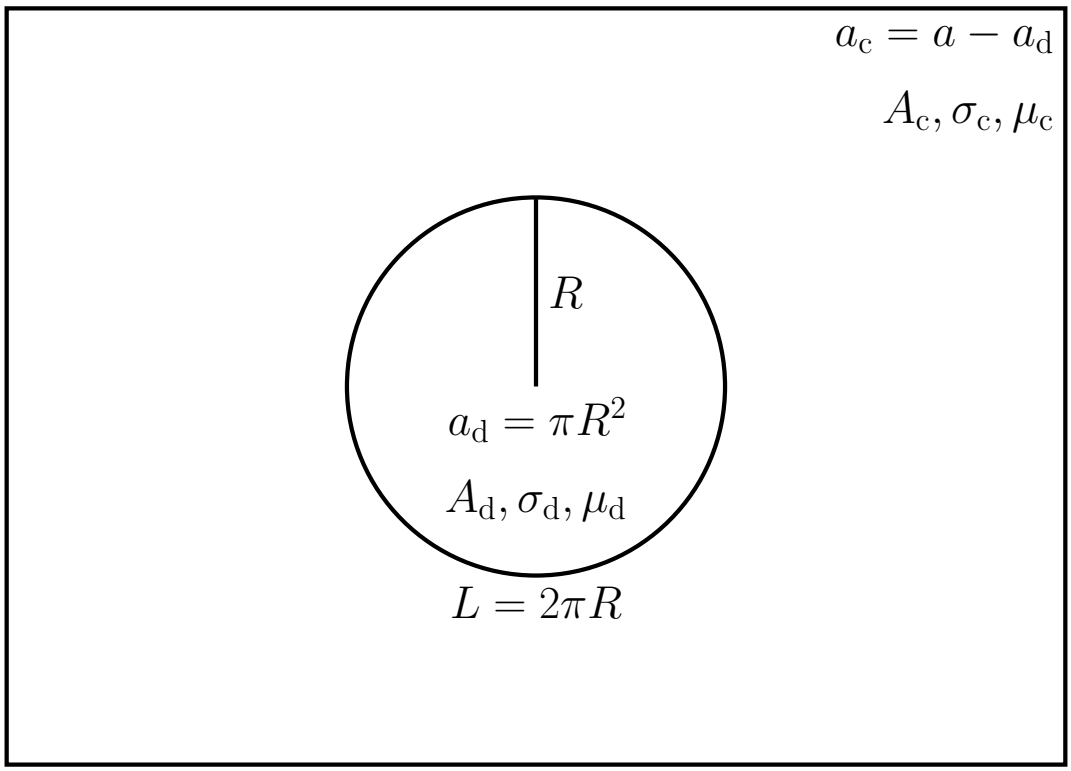

Figure S3: A sketch of a heterogeneous monolayer with a single circular domain (d) dispersed in the continous phase (c).

tension disappear and the system behaves as in Figure S2. In order to add the correction predicted by equation S11 to the isotherm, the average area per molecule $A = a/(N_c + N_d)$ needs to be related to R. From geometric consideration that is

$$A = \frac{aA_cA_d}{(a - \pi R^2)\, A_d + \pi R^2 A_c} \tag{S12}$$

Finally, we need to consider the relationship between τ and R. We can use the famous Tolman equation [1] for the dependence of the surface tension on the radius of a spherical droplet by substituting σ with τ:

$$\tau = \frac{\tau_0}{1 + 2\delta/R}, \tag{S13}$$

where τ_0 is the line tension at zero curvature (infinite radius) and δ is the Tolman length (in the order of ~ 3 Å). At radii approaching δ the equations break down and further elaboration is needed. The predictions of equation S11 are presented in Figure S4, starting from a cluster of 19 particles up to a $a_d = a/2$. As it can be seen the correction looks quite similar to what is observed from the simulation. Close to the terminal points of the process, the deviation of interfacial tension from the equilibrium is quite large compared to what is observed from the simulation. This is a function of the unrealistic lower limit (cluster of only 19 particles) for the validity of the equations. Figure 2a in the main text shows multiple domains of arbitrary shape. It can be easily shown that dividing up the domain into smaller circular domains, the relationship $\Pi(A)$ remains similar. However, in that case, the interfacial pressure approaches Π_{eq} slower, because of the smaller size of the domains.

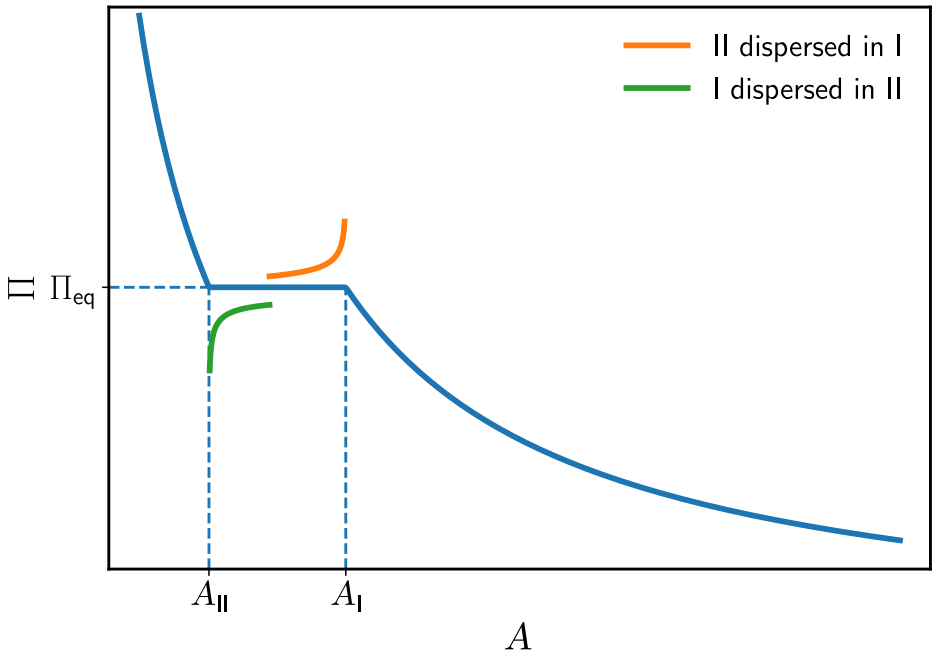

Figure S4: The addition of the line tension correction according to equations S11, S12 and S13 superimposed over the simple compression isotherm; $\Pi_{eq} = 16.3$ mN/m, $A_{I} = 43.6$ Å^2, $A_{II} = 34.6$ Å^2, $\tau = 1$ pN, $\delta = 3$ Å, $R_{min} = 12.2$ Å and $a = 256$ nm^2

3 2D orientational order parameter

In the main text, the orientational order parameter is computed in three dimensions. The z axis (the interface normal) is chosen as the natural director vector for the surfactants and is used to define the angle θ between the surfactant's principal axis and the director. Here, we also consider the 2D case where the projection of the principal axis in the xy-plane is used. The projection is illustrated in Figure S5, obtaining the vector $\mathbf{p}^{2D}$. This requires a more general method in which the director vector is not known in advance[2, 3].

Firstly, the order parameter tensor is calculated as

$$\mathbf{Q}_{\alpha\beta} = \frac{1}{N}\sum_{i}^{N}\left(\frac{d\mathbf{p}_{i\alpha}\mathbf{p}_{i\beta} - \delta_{\alpha\beta}}{d-1}\right) , \tag{S14}$$

where $\mathbf{p}_i$ is the (normalized) principal axis of molecule i, d is the number of dimensions, N the number of molecules, and α/β are the Cartesian indices. Having obtained the tensor $\mathbf{Q}_{\alpha\beta}$, the order parameter is the largest positive eigenvalue of $\mathbf{Q}_{\alpha\beta}$ and the director is the corresponding eigenvector. The data in Table S1 shows that the 2D orientational order parameter for 7:1 FTOH is small for a range of areas per molecule spanning the LE-C transition.

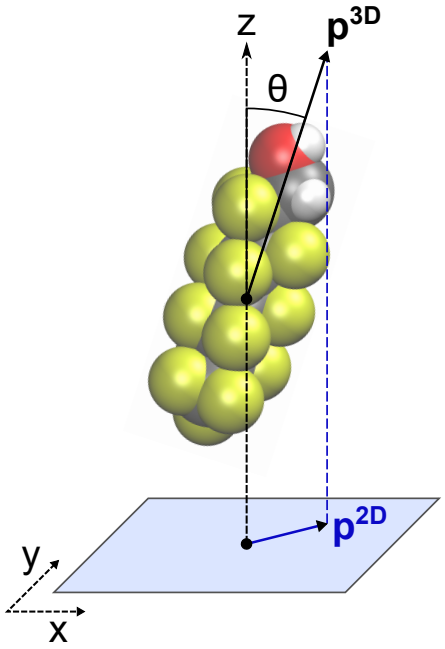

Figure S5: Projection of surfactant's principal axis $\mathbf{p}^{3D}$ (denoted $\mathbf{p}_1$ in the main text) onto the xy-plane as used in computation of 2D orientational order parameter. Note: The 2D vector $\mathbf{p}^{2D}$ is normalized after projection.

Table S1: 3D and 2D (x,y) orientational order parameters computed for 7:1 FTOH at different areas per molecule and 293 K

	Order parameter	
Area/molecule [Å^2]	3D	2D (x,y)
28	0.905	0.057
30	0.896	0.059
35	0.764	0.060
40	0.605	0.059
50	0.433	0.066

4 Supplementary Figures and Tables

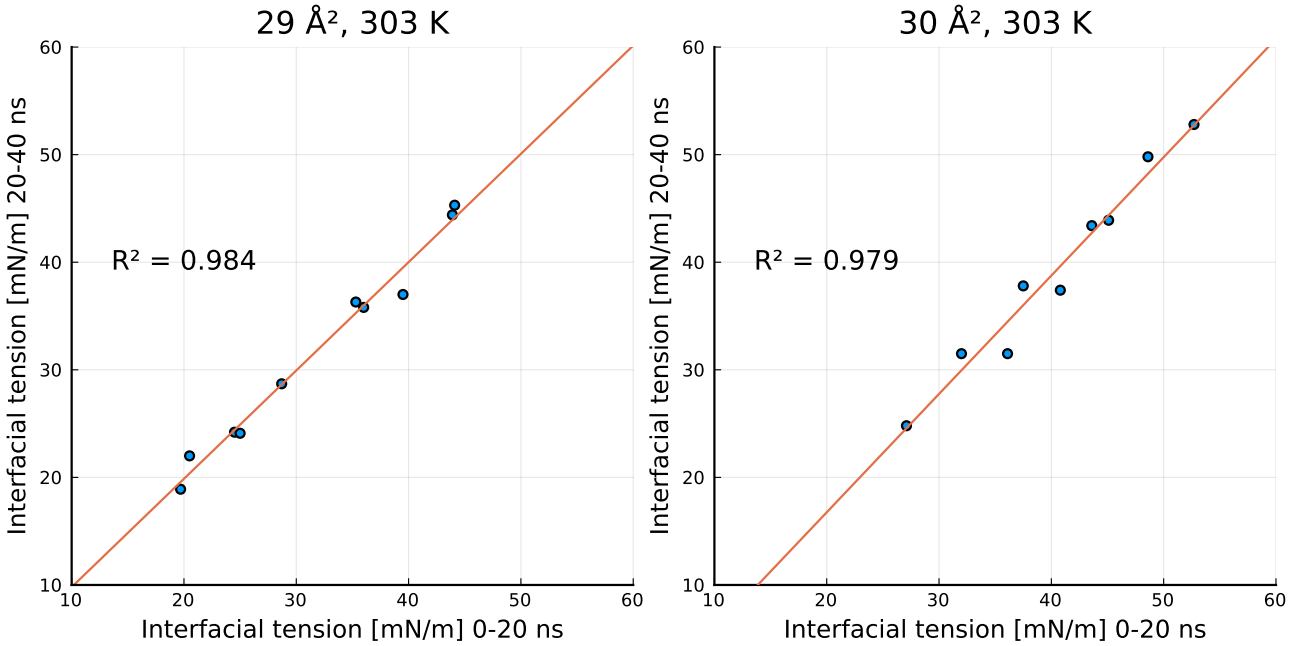

Figure S6: Correlation between interfacial tension measured in the first half (0-20 ns) and second half (20-40 ns) of extended simulations of 7:1 FTOH monolayers. Each point represents one independent 40 ns simulation.

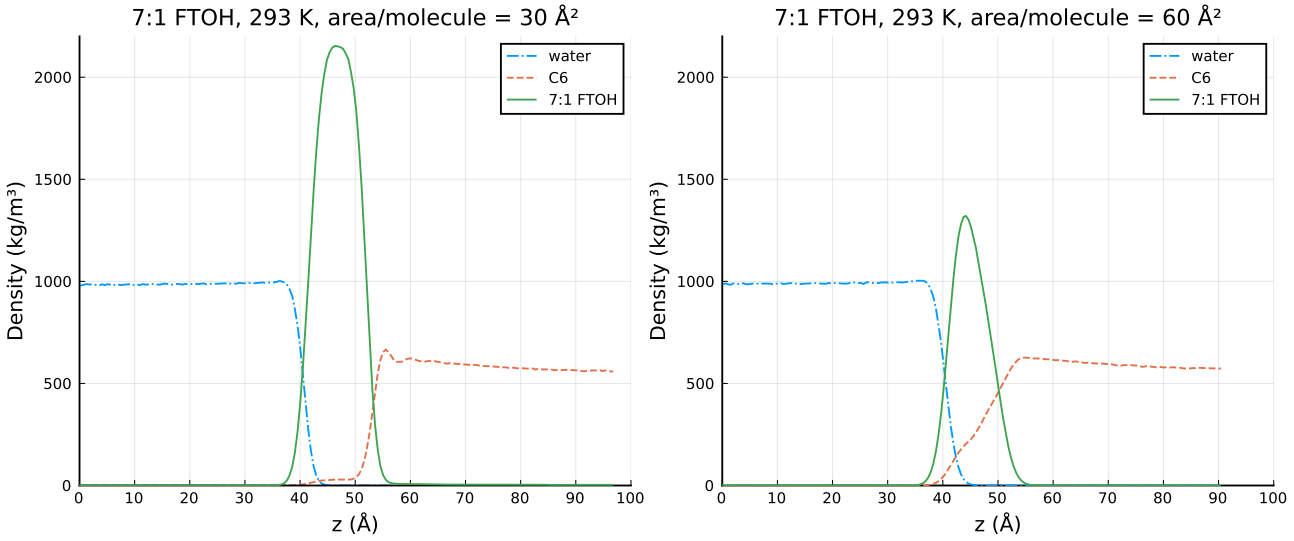

Figure S7: Density profile $\rho(z)$ of each component at the interface. $z = 0$ is defined as the mid-point of the water layer and the interface normal is parallel to $\vec{z}$.

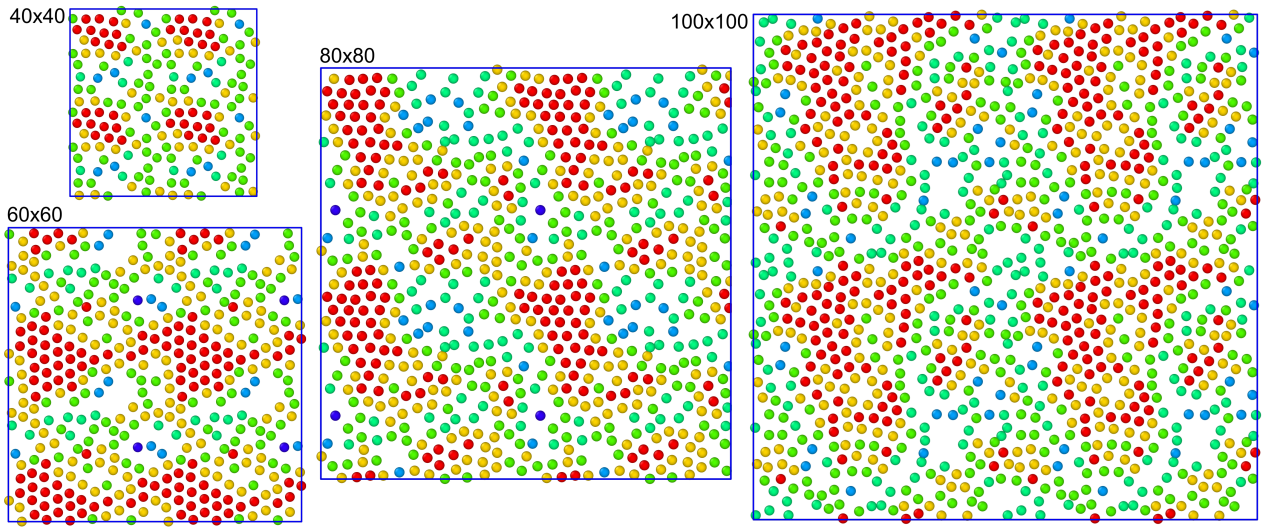

Figure S8: Visualization of crystalline cluster size in simulations at 36 Å^2/molecule and 303 K for different simulation box sizes. Labels are the x/y box dimension (Å).

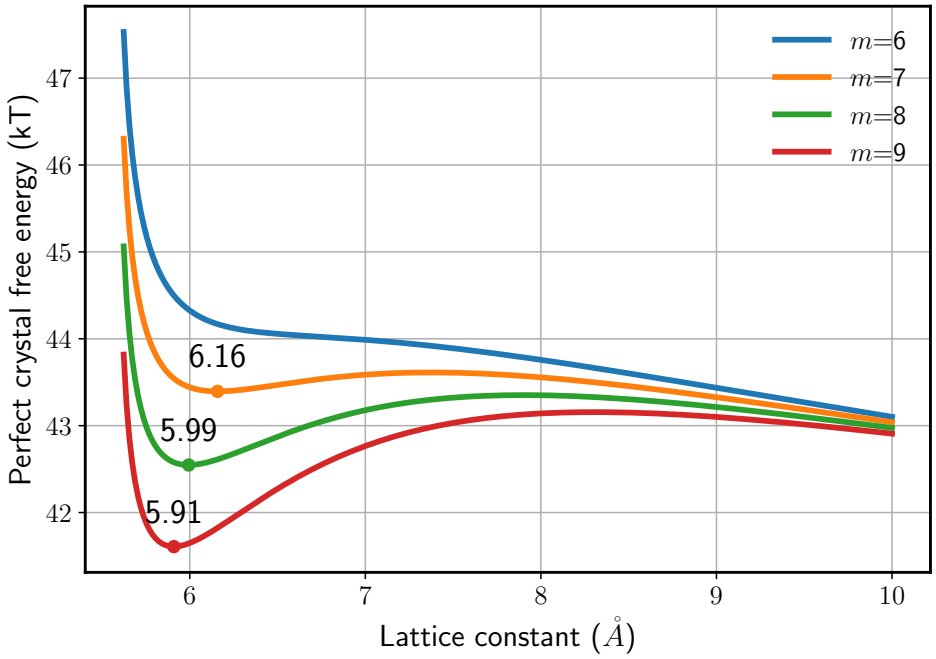

Figure S9: The free energy per molecule of a hypothetical perfect 2D van der Waals crystal as a function of the lattice constant d at different F-block lengths. $\alpha_{\text{free}} = \pi \left(d/2 - \sqrt{\alpha/\pi}\right)^2$, $T = 20^{\text{o}}$C, $\alpha = 24.5$ Å^2, $l_{\text{CF}_2} = 1.3$ Å, $L_{\text{CF}_2} = 10.5\text{x}10^{-78}$ Jm^6.

Table S2: Dependence of computed water/hexane interfacial tension on temperature

temperature [K]	σ_0 [mN/m]
283	55.23 ± 0.51
293	54.88 ± 0.32
303	54.38 ± 0.29
313	54.29 ± 0.21
323	53.45 ± 0.22

Table S3: Dependence of computed water-hexane interfacial tension on Lennard-Jones cutoff distance (293 K)

cutoff [nm]	σ [mN/m]
1.3	54.88 ± 0.32
1.5	55.17 ± 0.24
1.7	55.06 ± 0.29
1.9	54.91 ± 0.37
2.1	55.18 ± 0.71

Table S4: Effect of x/y box size on computed interfacial pressure, Π, at 36 Å^2/molecule for 7:1 FTOH

T [K]	area/molecule [Å^2]	x/y size [Å]	Π [mN/m]
303	36	40	18.52 ± 0.57
		60	17.86 ± 0.62
		80	17.17 ± 0.68
		100	16.66 ± 0.44
		120	16.42 ± 0.41
313	36	40	20.80 ± 0.81
		60	18.96 ± 0.56
		80	19.10 ± 0.50
		100	18.73 ± 0.52
		120	18.97 ± 0.57

References

[1] Richard C Tolman. The effect of droplet size on surface tension. *The Journal of Chemical Physics*, 17(3):333–337, 1949.

[2] R Eppenga and Daan Frenkel. Monte carlo study of the isotropic and nematic phases of infinitely thin hard platelets. *Molecular physics*, 52(6):1303–1334, 1984.

[3] Mark R Wilson. Determination of order parameters in realistic atom-based models of liquid crystal systems. *Journal of Molecular Liquids*, 68(1):23–31, 1996.